J Appl Electrochem (2013) 43:1117–1129
DOI 10.1007/s10800-013-0560-3

ORIGINAL PAPER

Effect of cation-exchange layer thickness on electrochemical and transport characteristics of bipolar membranes

Victor Zabolotskii · Nicolay Sheldeshov · Stanislav Melnikov

Received: 29 January 2013 / Accepted: 8 May 2013 / Published online: 26 May 2013

Abstract To study the effect of cation-exchange layer thickness on the electrochemical and transport characteristics of bipolar membranes (BPM), asymmetric BPM with varied cation-exchange layer thickness (of 10, 30, 50 and 70 μm) were investigated. High influence of BPM monopolar layers thickness on its selectivity had been shown. This fact is non-trivial in relation to monopolar ion-exchange membranes as their selectivity does not depend on their thickness. At the same time, increase or decrease in the thickness of BPM monopolar layers can increase products purity or, on the contrary, combine ion transport and pH shift functions.

Keywords Bipolar membrane · Current–voltage characteristic · Electrochemical impedance · Equivalent circuit · Warburg impedance · Gerisher impedance · Transport numbers · Water dissociation

List of symbols

T_i	Effective transport number of ion
t_i^m	Electromigration transport number of ion
P_i	Diffusive permeability of the membrane to ion (mol/cm^2 s)
ΔC_i	Concentration difference on the inlet and outlet of cell (mol/L)
i	Current density (mA/cm$^{2)}$
S	Membrane active area (cm^2)
R_b	Resistance of the reaction layer (Ohm cm^2)
R_0	Real part of impedance at low frequency (Ohm cm^2)
R_∞	Real part of impedance at high frequency (Ohm cm^2)
R_{wd}	Resistance of the space charge region (Ohm cm^2)
η_b	Bipolar region overvoltage (V)
U	Voltage (V)
U_w	Operating voltage at which water dissociation occurs (V)
j_i	Flux of ions (mol/cm^2 s)
d_{CEL}	Thickness of cation-exchange layer (microns)
D_i	Diffusion coefficient of ion inside the membrane (m^2/s)
χ	Effective water dissociation constant (s^{-1})
ω	Angular frequency
Z_G	Gerischer impedance
Z_W	Finite Warburg impedance
Z_{sp}	Impedance of the space charge region

1 Introduction

Bipolar membranes (BPM) are bilayer composites, in which cation- (CEL) and anion-exchange (AEL) layers possess ion-selective properties. Bipolar membranes occupy a special place among ion-exchange membranes due to their ability to generate protons and hydroxyl ions from water molecules under direct current polarization. Water dissociation occurs in bipolar region (a place where CEL and AEL are conjoined) of BPM only when its cation-exchange layer faces the cathode and anion-exchange the anode (the so-called generation mode) (Fig. 1). Thus, BPM can be viewed as an electrochemical reactor, which has functions of reaction product separation and their output beyond the reaction zone.

V. Zabolotskii · N. Sheldeshov · S. Melnikov (✉)
Kuban State University, Stavropolskaya 149, 350040 Krasnodar, Russia
e-mail: melnikov.stanislav@gmail.com

V. Zabolotskii
e-mail: vizab@chem.kubsu.ru

N. Sheldeshov
e-mail: sheld_nv@mail.ru

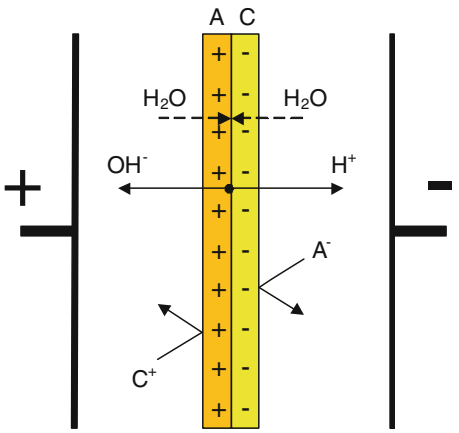

Fig. 1 Scheme of bipolar membrane function. *A* anion-exchange layer of the bipolar membrane, *C* cation-exchange layer, A^- salt anion, C^+ salt cation

These properties allow designing a number of unique electromembrane processes, which have huge industrial impact. These processes include acids and bases synthesis [1–6], electrochemical regeneration of acidic and basic gas sorbents [7, 8] and ion-exchange resins [9], protein separation [10, 11], pH correction of natural waters [12] and juices [13].

The main characteristics that define the possibility of BPM effective application are bipolar region overvoltage, total potential drop across the membrane and water dissociation current efficiency. These three parameters are closely related to each other and determined by physical structure of monopolar layers and chemical nature of water dissociation reaction catalyst placed in the bipolar region.

As with any other type of ion-exchange membranes, some amount of salt ions (in case of BPM they are co-ions) are present inside the monopolar layers of BPM. Their presence leads to contamination of the final products (acids and bases) by salt ions. In general, the number of salt ions that come into acid and into alkali is different, that is, flux of salt ions through the bipolar membrane during electrodialysis is asymmetrical [14, 15]. It is possible to control this process by changing the thickness of the monopolar layers of bipolar membrane [15, 16]. Membranes, with different thicknesses of CEL and AEL will be called asymmetric bipolar membranes.

As it was shown in a number of papers [17–19], for formation of bipolar region it is enough to apply very thin (10–50 μm) CEL on the surface of anion-exchange membrane. Application of different antipolar layers on monopolar membrane substrate such as thin films [15, 19] saves the high permeability of one of the layers (anion-exchange [15] or cation-exchange [19]) for the salt ions, and at the same time, such a membrane acquires the ability to effectively dissociate water due to the formation of a bipolar region. The advantage of these membranes is the ability to adjust the ratio of the salt ions and water dissociation products transport by adjusting the thickness of one of the layers that make up a bipolar membrane or applied current density.

However, optimal CEL thickness for various electromembrane processes remains unclear. Selection of the proper thickness of cation-exchange layer will provide a membrane with selective properties similar to the classic bipolar membranes or capable of simultaneous generation of water dissociation products and transport of salt ions. Additionally, it is interesting to find out contribution of the monopolar layer thickness and CEL, in particular in total voltage drop across the bipolar membrane.

2 Experimental

2.1 Asymmetric bipolar membranes formation

To obtain mechanicaly stable asymmetric bipolar membrane the CEL (sulfonated polytetrafluoroethylene membrane MF-4SK) film was applied on the surface of a heterogeneous membrane containing polyethylene, by the method used in [20]: the surface layer of a heterogeneous anion-exchange membrane was pretreated with acetic acid, after which the MF-4SK solution (4 % mass in dimethylacetamide/acetic acid solution) was applied to the surface of the anion-exchange substrate–membrane. The use of acetic acid causes swelling and expansion of the polyethylene chains; thus, there is a weave of hydrophobic chains of polyethylene with the hydrophobic part of the sulfonated polytetrafluoroethylene matrix to form a new intermediate layer, which is due to the presence of a hydrophobic part has high adhesion with the hydrophobic part of the MF-4SK and with its polar part with the substrate–membrane.

Comparative characteristics of monopolar layers forming an asymmetric bipolar membrane are shown in Table 1.

Asymmetric bipolar membrane with a CEL thickness of 10, 30, 50 and 70 μm was created in order to study the effect of a CEL thickness on the electrochemical and transport characteristics of the bipolar membrane. Obtained experimental results were compared with the data obtained for heterogeneous ion-exchange membrane MB-2 [21], with CEL thickness of 450 μm (Table 2).

2.2 Experimental setup

The measurements were carried out in a four-compartment electrochemical cell (Fig. 2) with active membrane area of 2.27 cm^2. Membrane under study was separated by monopolar membranes from the polarizing platinum electrodes, to avoid contact with the products of the electrode reactions. The impedance spectra were obtained with platinized platinum electrodes made of platinum wire with

Table 1 Properties of monopolar layers forming an asymmetric bipolar membrane

Properties	Cation-exchange layer	Anion-exchange layer
Membrane	MF-4SC	Ralex AMH-Pes
Polymer base	Polytetrafluoride ethylene	Polystyrene divinylbenzene
Ionogenic groups	$R-SO_3^-$	$R–N^+(CH_3)_3$
Inert binder	–	Polyethylene
Reinforcing fabric	–	Polyester
Wet thickness (mm)	0.01–0.07[a]	0.45
Counterion transport number (1.0/0.5 M NaCl)	>0.94	>0.95
Ion-exchange capacity, mmol/g-dry	0.7–0.8	1.8

[a] Cation-exchange layer thickness was set individual for each membrane

Table 2 Properties of heterogeneous bipolar membrane [21]

Ionogenic groups	
Cation-exchange layer	$R–SO_3^-$
Anion-exchange layer	$R–N^+(CH_3)_3$
Ion-exchange capacity $N_{\pm}$, mol-eq/L	
Cation-exchange layer	1.4
Anion-exchange layer	1.4
Thickness, mm	>1.0
Transport number	
in 0.5 M solution of sodium hydroxide	0.16
in 0.5 M solution of hydrochloric acid	0.01
Current efficiency, %	
Acid	86
Alkali	94
Voltage drop[a], V	12.9

[a] Measured in 0.5 M NaCl at 20 mA/cm^2

a diameter of 0.1 mm, located at a fixed distance from the surface of the membrane. For the measurement of current–voltage curves (CVC), Luggin–Haber capillaries connected to Ag/AgCl electrodes were used.

The electrochemical cell and feed solutions are shown in Fig. 2.

Cation-exchange layer of studied BPM was in contact with 0.01, 0.1 or 0.5 M solution of hydrochloric acid, anion-exchange layer—with sodium hydroxide solution of the same concentration. Acid and alkali solution flow rate was set constant at 2 ml/min. This membrane setup is favoring for the establishment of conditions similar to working ones [28].

All experiments were carried out at 25.0 ± 0.1 °C.

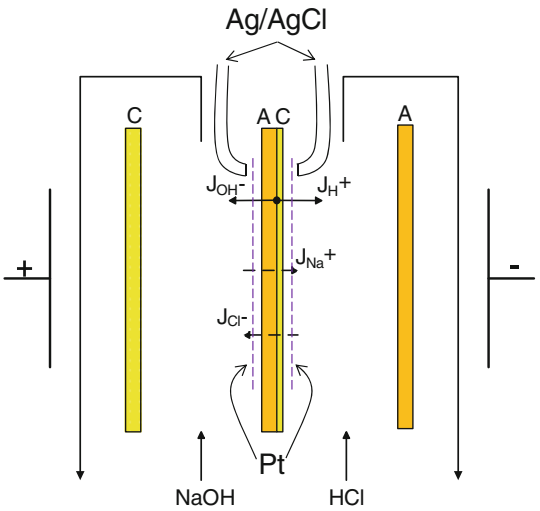

Fig. 2 Scheme of the experimental cell and the flow of ions through the membrane under investigation. *A* anion-exchange membrane/layer; *C* cation-exchange membrane/layer; *Pt* platinized platinum wire used for impedance measurement; Ag/AgCl electrodes connected with Luggin-Gabber capillary for CVC measurement

2.3 Voltammetry

The current–voltage characteristic of the bipolar membrane allows evaluating such important, for practical application, characteristics as limiting electrodiffusion current density and operational voltage. As in the case of monopolar membranes, the main charge carriers within the ohmic region of bipolar membranes' CVC are salt ions, and reaction of water dissociation does not occur. Further increase in applied current density (above the limiting value) leads to salt ions removal from bipolar region (limiting current plateau), formation of space charge and start of water dissociation reaction (leads to overlimiting, that is, water dissociation, current). The later factors result in CVC deviation from linearity of limiting current plateau. The following rise in current appears exclusively due to water dissociation reaction and can be addressed to flux of H^+ and OH^- ions [14, 15, 22]. For bipolar membrane, close to the ideal [23, 24], the water dissociation potential must be close to 0.6–0.8 V and practically does not change with increasing current density. The most detailed correlation of the different regions of the bipolar membranes' CVC to the proceeding process is described in [15].

In the present study, dynamic method was used for measuring the current–voltage characteristic of asymmetric bipolar membranes. Membrane under study was placed for 30–40 min in an electrochemical cell, described above, without applying polarizing current. After that, linearly increasing and decreasing current was applied to the cell and CVC recorded. Current sweep rate was set at 2×10^{-5} A/s, which gives a minimal hysteresis sweep between forward and backward CVCs.

2.4 Transport numbers

Non-selective transport of ions across the BPM occurs due to two mechanisms—their diffusion and migration—and can be described by the equation:

$$T_i = t_i^{\mathrm{M}} + \frac{P_i \Delta c_i F}{iS} \quad (1)$$

where the first term is the migration transport number of the ion and the second term the contribution of the diffusion component.

Thus, the calculation of the mean value of the electromigration transport number across the membrane and the diffusion permeability coefficient is reduced to the determination of the coefficients in the equation of the linear dependence in the coordinates "T_i–i^{-1}" (Fig. 3).

In this study, a modified Hittorf method adapted for measuring transport numbers in membranes was used. The aim of the method is to determine the total flux of sodium cations into the acid from alkali and total flux of chlorine anions into the alkali from acid.

The experimental setup is described above in Sect. 2.2. For measurement of ions transport numbers, the constant current density was applied to the cell. The electrochemical system was kept at a given current density for 1 h. After that, three samples of 25 ml were taken from each compartment (acid and alkali) with time interval of 30 min. In these samples, the concentrations of chloride anion (in alkali) and sodium cation (in acid) were measured. The resulting transport number value was calculated using mean ion concentration between these three.

The concentration of chloride ions in the sodium hydroxide solution was determined by potentiometric titration with silver nitrate solution, and the solution was neutralized with nitric acid prior to titration. The concentration of sodium ions in the hydrochloric acid solution was determined potentiometrically. In addition, the concentrations of chloride ions in the sodium hydroxide solution and sodium ions in the hydrochloric acid solution, which was fed to the cell, were measured.

Effective transport numbers of sodium and chloride ions across bipolar membrane were calculated by the equation:

$$T_{\mathrm{Na^+,Cl^-}} = \frac{\left(c_{\mathrm{Na^+,Cl^-}} - c^0_{\mathrm{Na^+,Cl^-}}\right) v_{\mathrm{Na^+,Cl^-}} F}{I} \quad (2)$$

Effective transport numbers of H^+ and OH^- ions across bipolar membrane were calculated by the equation:

$$T_{\mathrm{H^+,OH^-}} = 1 - (T_{\mathrm{Na^+}} + T_{\mathrm{Cl^-}}) \quad (3)$$

where $c_{\mathrm{Na^+,Cl^-}}$ и $c^0_{\mathrm{Na^+,Cl^-}}$—concentrations of ions in solution, coming from the cell, and in feed solution, mol/L; $v_{\mathrm{Na^+,Cl^-}}$—volume flow rate, L/s; F—Faradey constant, 96485 C/mol; I—current, applied to the cell, A; $T_{\mathrm{Na^+,Cl^-}}$—effective transport numbers of sodium and chloride ions; $T_{\mathrm{H^+,OH^-}}$—effective transport numbers of H^+ and OH^- ions.

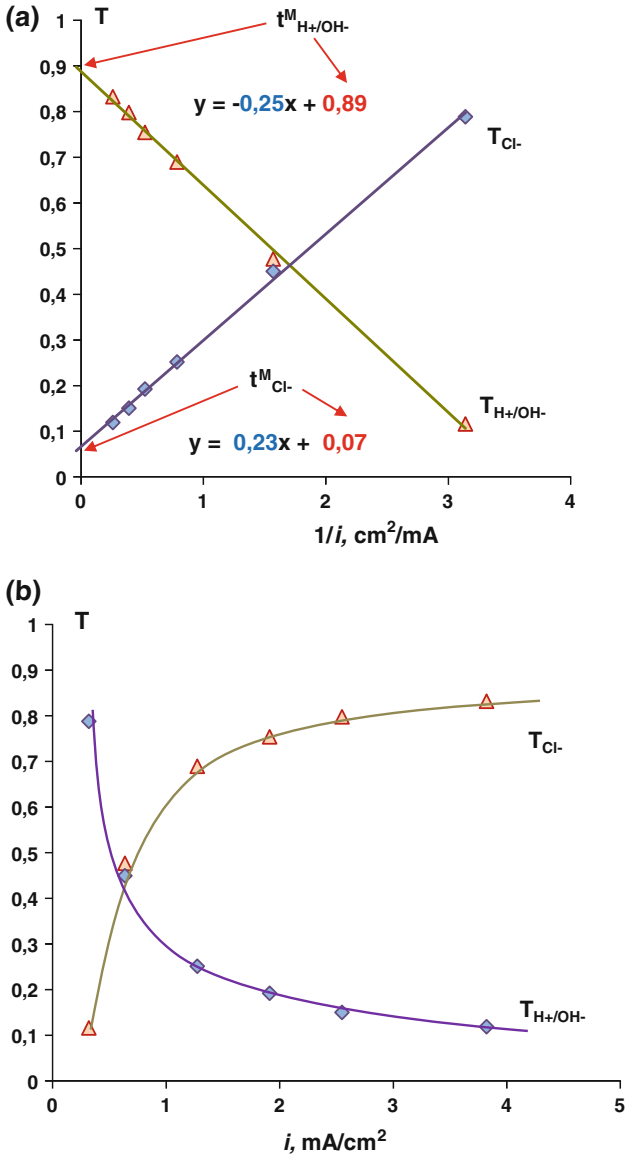

Fig. 3 Effective transport number of water dissociation products T_{H^+/OH^-} and chloride anions T_{Cl^-} versus reverse current density (**a**) and current density (**b**)

2.5 Electrochemical impedance spectroscopy

One of the first works devoted to electrochemical impedance spectrum of bipolar membranes treatment was done by Sheldeshov, Gnusin and Zabolotskii [25]. This method provides the most complete information on the processes of ion transport through a bipolar membrane under direct current polarization.

An example of electrochemical impedance spectrum of bipolar membrane is shown in (Fig. 4). At point **A,** the limit of the impedance spectrum of BPM at infinitely high frequencies ($\omega \to \infty$) is marked. From the value of the real component (R_∞) of the impedance at this point, one can estimate the total resistance of monopolar layers (CEL and AEL) of bipolar membrane, in other words ohmic part of membranes' total resistance. At point **B,** the limit of the impedance spectrum of BPM at infinitely low frequencies ($\omega \to 0$) is marked. From the value of the real component (R_0) of the impedance at this point, one can estimate the total resistance of BPM, including resistance occurring in the bipolar region due to water dissociation reaction.

Difference in the values of the real component of the impedance between points A and B (R_b) belongs to the bipolar region in which occurs a change in polarity of the ionic groups (in the transition from one monopolar layer to another), and localization of space charge and water dissociation occur. The emergence of this resistance causes the appearance of the potential "excess" (overvoltage) of the bipolar region and leads to the bipolar membrane CVC deviation from linearity as described above, in Sect. 2.4. The resistance of the bipolar region can be found as:

$$R_b = R_0 - R_\infty \tag{4}$$

Integrating the resulting dependences of R_0, R_b and R_∞ from the current density, one can build the partial CVCs of the membrane (U_m), bipolar region (η_b) and monopolar layers (U_0) [25] (Fig. 5), which cannot be obtained by other means.

$$\eta_b = \int_0^i R_b \, di \tag{5}$$

Electrochemical impedance frequency spectra measurements were carried out on virtual impedance meter coupled with computer, in the frequency range of alternating current from 3×10^{-6} to 1×10^{6} Hz

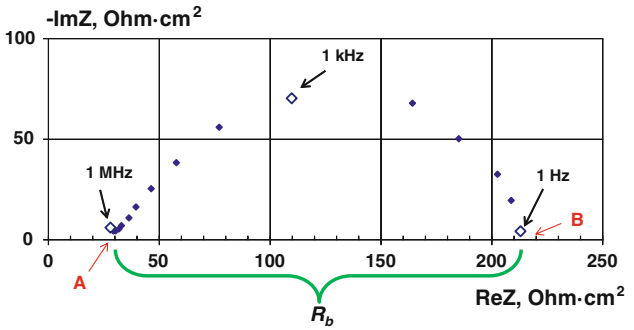

Fig. 4 Electrochemical impedance spectra of bipolar membrane under DC polarization with superimposed AC amplitude (example)

distributed uniformly in logarithmic scale. The amplitude of the AC was 200 mV. The choice of AC amplitude is a matter of compromise; it is determined by two conditions: The signal current should produce relatively small perturbations of concentrations and potential drop, and, on the other hand, the electrochemical noise should be avoided. The signal amplitude seems relatively high, which could result in a slight distortion of the signal when the DC approaches the limiting current plateau. We have, however, verified that the signal remains always very close to a sinusoid and harmonics are absent. It is difficult in experiment to reduce the AC amplitude without degradation of the signal quality and appearance of the noise.

Prior to main measurements, a series of measurements on sodium chloride solution were made without membrane to estimate an ohmic part of the measured impedance. These measurements shown that the ohmic contribution of total impedance is equal to 4 Ohm·cm^2 for real and imaginary parts of impedance. The relative error magnitude of impedance measurements was less than 1 %.

3 Results and discussion

3.1 Electrochemical characteristics of asymmetric bipolar membranes

Heterogeneous anion-exchange membrane surface lamination with MF-4SK film leads to sharp drop in value of the limiting electrodiffusion current density compared to the initial membrane–substrate, which can be seen from the general current–voltage characteristics (Fig. 6). CEL with

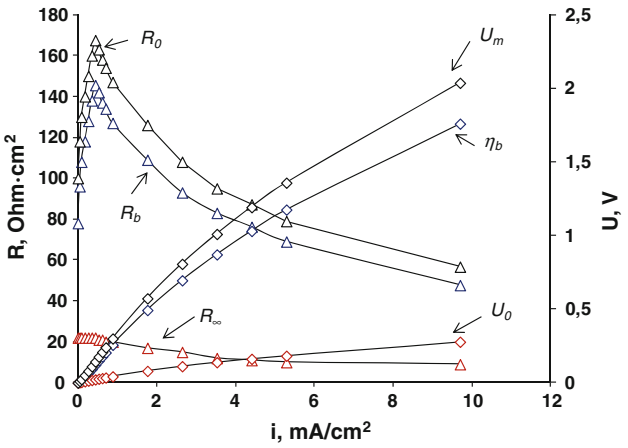

Fig. 5 Ohmic (R_∞), bipolar region (R_b) and total membrane (R_0) parts of impedance real component and partial CVCs of the membrane (U_m), bipolar region (η_b) and monopolar layers (U_0). Data shown were obtained for industrial heterogeneous bipolar membrane MB-3

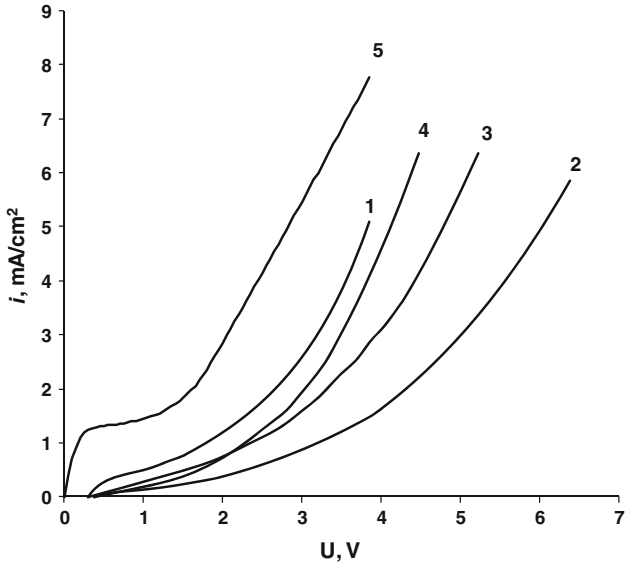

Fig. 6 General current–voltage characteristics of asymmetric bipolar membrane with CEL thickness, μm: 1–10, 2–30, 3–50, 4–70, 5–0 (initial anion-exchange membrane). The concentration of acid and alkali solutions—0.01 M. An ohmic drop between capillaries and membrane surface (53.5 mV) is included

a 30 micron thickness reduces the value of the limiting current down to 0.05 mA/cm^2, against 1.2 mA/cm^2 for the initial anion-exchange membrane measured under the same conditions. Obviously, this effect is caused by highly selective MF-4SK layer, which "locks" the anion-exchange surface, interfering anions transport across resulting bipolar membrane. As a result, anions may transfer only by diffusion through CEL and after passing the bipolar border by diffusion and migration through AEL. In this case, thin CEL may be viewed as a diffusion layer for anions with constant thickness.

A decrease in the operating voltage (U_w) on asymmetric bipolar membrane with simultaneous CEL thickness increase can be seen from obtained general CVCs (Fig. 6; Table 3). This phenomenon can be explained as follows: In the absence of highly active water dissociation reaction catalyst in the bipolar region, the total flux of water dissociation products is strongly affected by the value of bipolar region overvoltage. However, this value is highly dependent on a ratio of ion-exchange groups in bipolar region in salt and hydroxyl or proton form as stated in [26]. Thus, increase in CEL thickness leads to smaller flux of anions through membrane and increase in the overvoltage value that increases the resulting flux of protons and hydroxyl ions.

In our case, diffusion of anions to bipolar border, for membranes with CEL thickness of 30 microns, reduces the electric field strength and BPM water-splitting capability. On the other hand, high selectivity of asymmetric bipolar membranes with CEL thickness bigger than 50 microns leads to an absence of salt ions on the bipolar border, increasing electric field strength, promoting water dissociation reaction and reducing potential drop across BPM. The asymmetric membrane stands out of this dependence, due to the fact that its transport properties are closer to those of the monopolar membrane than the bipolar as shown by its electromigration transport numbers of chlorine anion (Table 3).

The results of transport number measurement confirm the conclusions based on the measurement of current–voltage characteristics of the membrane: with increasing thickness of the CEL transport number of chloride ions through it decreases (Fig. 7a). Moreover, at a film thickness of MF-4SK of about 50 microns and above, the differences in transport numbers between membranes with different CEL thickness are insignificant and their values are close to the values characteristic of heterogeneous bipolar membrane. Consequently, sodium ion leakage through the AEL of the BPM, characterized by its transport number T_{Na^+}, remains constant at 5 ± 2 %, because sodium ion transport is completely determined by AEL properties which are the same for all investigated membranes.

On the contrary, the amount of chloride ion leakage j_{Cl-} through the CEL is significant (Fig. 7b). Furthermore, it is apparent that flux of chloride ions reaches a limiting value at different current densities depending on the CEL thickness, with exception of membrane with CEL thickness of 10 microns. In the latter case, it means that the co-ion leakage through thin CEL remains at current densities when water dissociation reaction occurs. For the membranes with CEL thickness greater than 10 microns, no overlimiting current of co-ions is detected at this current density. Thus, no electroconvection effect or water-

Table 3 Electromigration transport numbers of ions and water dissociation potential for asymmetric bipolar membranes with different CEL thickness

CEL thickness, μm	10	30	50	70	450
t^m_{Na+}	0.05 ± 0.02	0.05 ± 0.02	0.05 ± 0.02	0.05 ± 0.02	0.06 ± 0.02
t^m_{Cl-}	0.14 ± 0.03	0.09 ± 0.02	0.06 ± 0.01	0.05 ± 0.01	0.05 ± 0.01
$t^m_{H+/OH-}$	0.81 ± 0.05	0.85 ± 0.04	0.89 ± 0.03	0.91 ± 0.03	0.89 ± 0.03
U_w, V	2.5	4.1	3.3	2.9	2.2

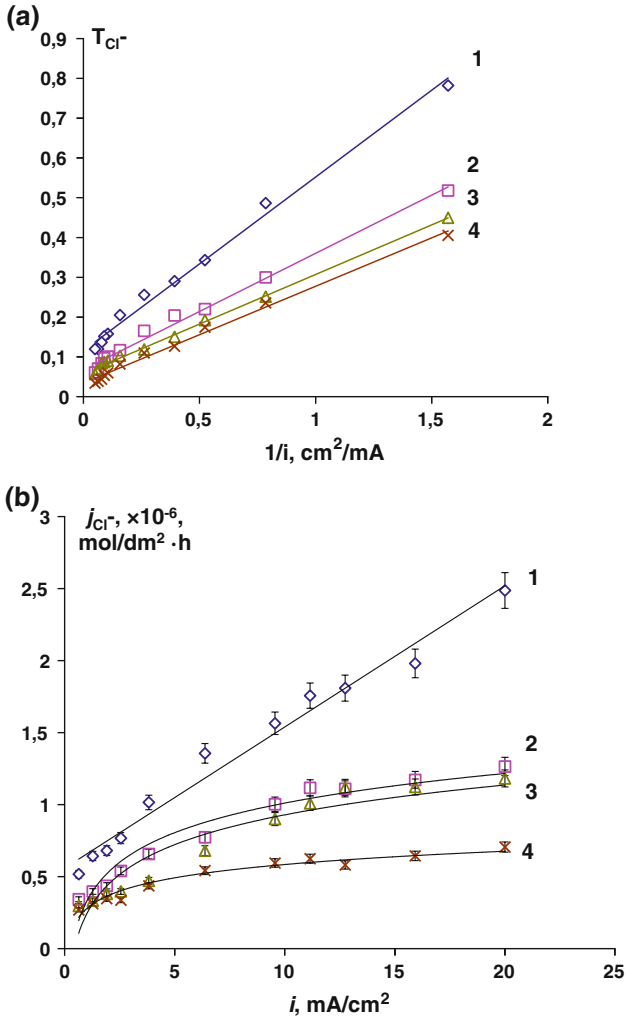

Fig. 7 Transport numbers of chloride ions versus reverse current density (**a**) and flux of chloride ions versus current density (**b**) through the asymmetric bipolar membrane with CEL thickness, μm: 1–10, 2–30, 3–50, 4–70

splitting contribution at the CEL–solution interface affects the value of j_{Cl-}.

The effect of external solutions of various concentrations on electrochemical properties of asymmetric BPM is shown in Fig. 9 for membranes with CEL thickness of 30 microns. Spectra of electrochemical impedance (Fig. 9) measured for asymmetric bipolar membranes show the minimum value of the impedance at zero direct current density due to the presence of salt ions in the bipolar region. However, with the increase in the current density, impedance of the membrane is showing some difference from the ones described for industrial BPM [28]. The impedance spectra of studied membranes expand with increase in applied current density, which is associated with the withdrawal of salt ions (charge carriers) from the bipolar region. With further current density increase, reduction in bipolar region impedance appears to be due to increased flux of new charge carriers—H^+/OH^- ions. For industrial bipolar membranes, the expansion of spectra does not appear to be due to high water-splitting efficiency even at low currents.

Electrochemical impedance spectra of the asymmetric bipolar membrane with the CEL thickness of 30 micron in 0.1 M hydrochloric acid and sodium hydroxide (Fig. 9b) are not much different from the spectra obtained in 0.01 M solutions (Fig. 9a). However, the spectra obtained in a 0.5 M solution (Fig. 9c) show a distortion of the hodograph semicircle in the low-frequency range. This distortion can be explained in terms of equivalent circuit presentation.

To describe the electrochemical impedance spectrum of BPM, we will consider a one-dimensional bipolar membrane composed of anion-exchange layer and cation-exchange layer. The current flows through the membrane in the direction, leading to water dissociation. The bipolar membrane can be split into three zones: anion-exchange layer, bipolar interface and cation-exchange layer.

For simplicity, we will consider bipolar region as a one-dimensional sharp bipolar interface where reaction of water dissociation takes place. This assumption can be made considering that its thickness varies from 0.1 to 5–7 nm for different models [28, 29]. This order of magnitude is 10000 times smaller than the thickness of monopolar regions, which is 10–450 microns. However, it should be noted that in reality bipolar region itself includes multiple layers, as depicted in [28]: reaction layers and electric double layers in both AEL and CEL, local space charge region, and transition regions.

The overall water-splitting mechanism in the bipolar membrane can be described by a two-stage protonation–deprotonation reaction involving weak acid or weak base, which are ion-exchange groups or catalyst introduced to the bipolar region. This explanation of the water-splitting mechanism was given by Greben et al. [30] and Simons [31, 32].

In the case of weak acid, this reactions can be written as follows:

$$A + H_2O \underset{k_{-1}}{\overset{k_1}{\Leftrightarrow}} AOH^- + H^+ \tag{6}$$

$$AOH^- \underset{k_{-2}}{\overset{k_2}{\Leftrightarrow}} A + OH^- \tag{7}$$

and for weak base:

$$B + H_2O \underset{k_{-1}}{\overset{k_1}{\Leftrightarrow}} BH^+ + OH^- \tag{8}$$

$$BH^+ \underset{k_{-2}}{\overset{k_2}{\Leftrightarrow}} B + H^+ \tag{9}$$

Both reactions can be summarized in the following reaction:

$$H_2O \underset{k_{-1}}{\overset{k_1}{\Leftrightarrow}} H^+ + OH^- \tag{10}$$

In both the suggested mechanisms above, the second steps, thus either Eqs. (7) or (9), are rate determining. If one of these mechanisms is active in the reaction layer, the values of water dissociation rate constants k_1 and k_{-1} (Eq. (10)) become thus functions of the specific rate constants of Eqs. (7) or (9).

Solution for this problem was given by Gerischer in [34] for the case of metallic electrode/solution interface and later adapted for the case when water dissociation reaction occurs on ion-exchange groups of AEL by Zabolotskii et al. [25] and Hurwitz [28]:

$$Z_G = \frac{R_b}{\sqrt{2}}\left(\sqrt{\frac{1}{\sqrt{a}}+\frac{1}{a}} - j\sqrt{\frac{1}{\sqrt{a}}-\frac{1}{a}}\right) \tag{11}$$

where $a = \left(\frac{\omega}{\chi}\right)^2 + 1$ and R_b is resistance across the reaction layer.

Zabolotskii, Gnusin and Sheldeshov proposed an equivalent circuit, which includes an element of G—Gerischer impedance.

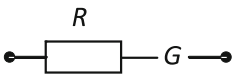

This scheme is good for description of the impedance spectra of the classic bipolar membranes [25].

In our case, high diffusion permeability of CEL with thickness of 10 and 30 microns leads to an ohmic region occurrence on general CVCs (Fig. 6, curves 1, 2). In addition, this can be clearly seen on total and partial bipolar region overvoltage current–voltage characteristics of asymmetric bipolar membrane with CEL thickness of 10 and 30 microns (Fig. 8, curves 1, 1′). A comparison of the partial and total current–voltage characteristics shows the same value of limiting current densities on the membrane and bipolar region. It is therefore reasonable to assume that Cl^- ion transfer across the CEL becomes a rate-limiting step in the transport of ions across asymmetric bipolar membrane on the contrary to transport through the diffusion layer at the CEL-solution boundary, as in the case of monopolar membranes. To describe the obtained impedance spectra (Fig. 9), an element of finite Warburg impedance (BW), which describes the diffusion of ions in the membrane systems [35], was consistently added in the existing scheme:

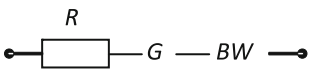

For simulation of finite Warburg impedance, we issued the Eq. (13), taken from [36] and adopted for membrane system.

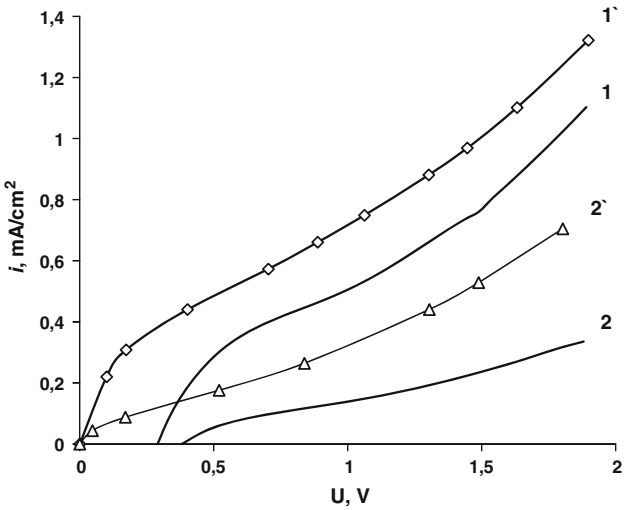

Fig. 8 The initial parts of the general (*1*, *2*) and partial bipolar region overvoltage (*1′*, *2′*) current–voltage characteristics for asymmetric bipolar membranes with CEL thickness of 10 (*1*, *1′*) and 30 (*2*, *2′*) μm

$$Z_W = \mathrm{A}(1-j)\tanh\left(W_c\sqrt{j\omega}\right) \tag{13}$$

where $A = \frac{W_s}{\sqrt{\omega}}$, W_s is the Warburg coefficient, $W_c = \frac{d_{CEL}}{\sqrt{D_{Cl^-}}}$, d_{CEL} is the thickness of CEL, D_{Cl-} is the diffusion coefficient of chloride ion in CEL.

It is worth recalling that because of water dissociation reaction taking place inside the BPM, it may be viewed as an electrochemical reactor. Such reactor may be formally associated with an internal resistance (R_{wd}) associated with the water-splitting reaction. Such treatment of the BPM impedance was made by Hurwitz and Dibiani in [28]. Following their steps, we also tried to introduce an element Z_{sp} consisting of capacitive contribution devoted to space charge region (C_{sp}) and a resistance R_{wd} referring explicitly to the water dissociation kinetics. Considering this, the experimental data were also fitted to the following equivalent scheme:

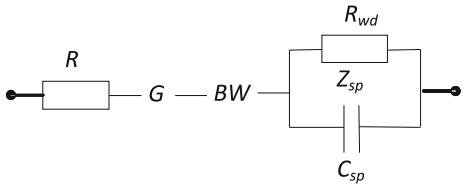

The expression for Z_{sp} may be found in [28]; rewriting using our notations, we obtain (Eq. (14)):

$$Z_{sp} = \frac{R_{wd}}{1+\left(R_{wd}\,C_{sp}\,\omega\right)^2} - j\,\frac{R_{wd}^2\,C_{sp}\,\omega}{1+\left(R_{wd}\,C_{sp}\,\omega\right)^2} \tag{14}$$

Taking into account the last equivalent scheme, the total impedance of the asymmetric bipolar membrane can be calculated as a sum of Eqs. (11) (13) (14):

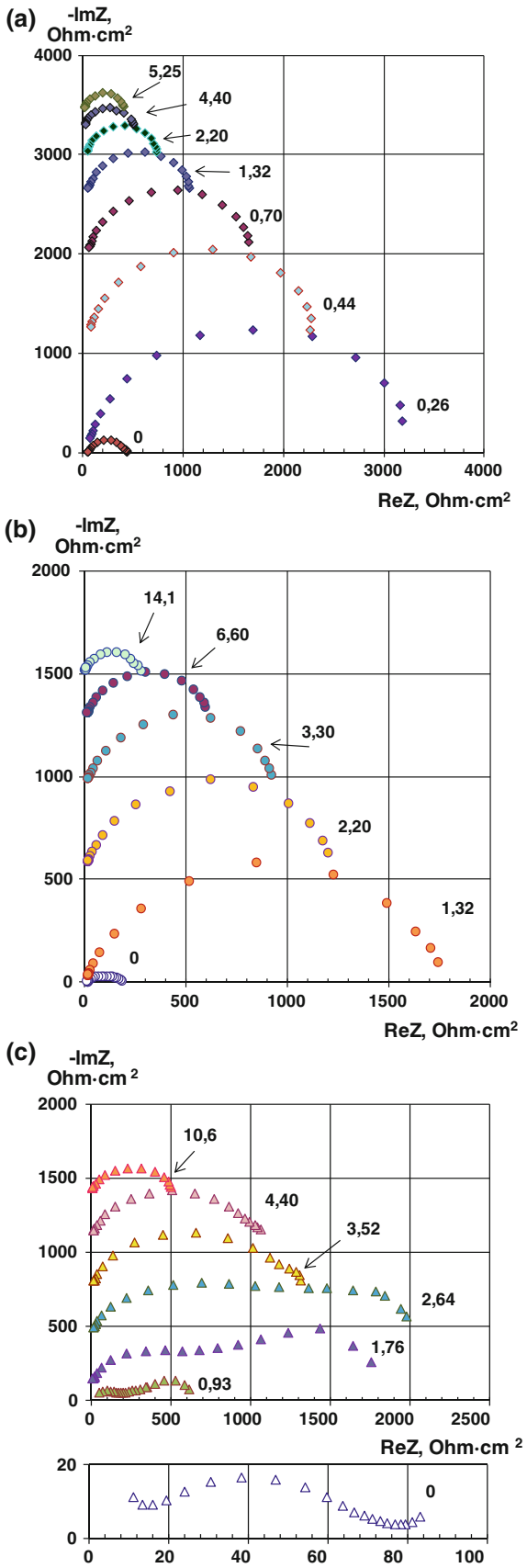

Fig. 9 Electrochemical impedance spectra for asymmetric bipolar membrane with CEL thickness of 30 microns. Concentrations of the solutions on both sides of the membrane are equal to 0.01 (**a**), 0.1 (**b**) and 0.5 M (**c**). The numbers next to the curves—the value of direct current density applied to the membrane. The spectra are shifted vertically relative to each other for clarity

$$Z_T = R + Z_G + Z_W + Z_{sp} \quad (15)$$

In Eq. (15), the first term define the total ohmic part of impedance associated with ohmic resistance of the bulk of AEL and CEL and resistance of the solution between measuring electrodes and membrane. The second term corresponds to the homogeneous chemical reaction—water dissociation reaction taking place in the bipolar border of BPM. The third term defines the non-selective transport of salt co-ions across transition (space charge) region in the bipolar border of BPM. The last term corresponds to the water dissociation product transport in space charge region. However, the equation (Eq. (11)) was derived under consideration that the electrical properties and ion concentrations in the bipolar region are unchanged and the external electric field across the reaction layer is reduced to zero [28]. Thus, it is also interesting to see whether the last term in Eq. (15) has an impact on the overall shape of the spectrum. To detect this effect we also tried to fit the experimental data with spectrum calculated considering only first three terms in Eq. (15).

The fitting of experimental data and calculated curves was made using numerical solution. To simplify the fitting procedure, first values of some parameters were taken from the experimental data. At first, the value of χ was calculated from the experimental impedance data, and then the value of R and first guess of the value R_b were added to the fitting parameters. The values for chloride ion diffusion coefficient inside transition region were taken as approximately 1×10^{-10} m^2/s, and the value for space charge capacitive contribution was taken as 2 μF. Parameters such as W_s and R_{wd} were then calculated. And all remaining parameters were fitted.

The results of fitting are shown in Fig. 10, and the values of different fitting parameters are shown in Table 4.

Comparison of experimental electrochemical impedance spectra with simulation results using the proposed equivalent circuits shows that both proposed schemes are adequate and can be used for qualitative description of the results (Fig. 10). In both cases, the value of dispersion between experimental data and fitting results is similar to each other. Some difference may be found in the first semicircle at low current densities, where we can see simultaneous action of several factors—electrochemical reaction (G) and capacitive current of the space charge region (Z_{sp}). Due to these fast rates of water dissociation

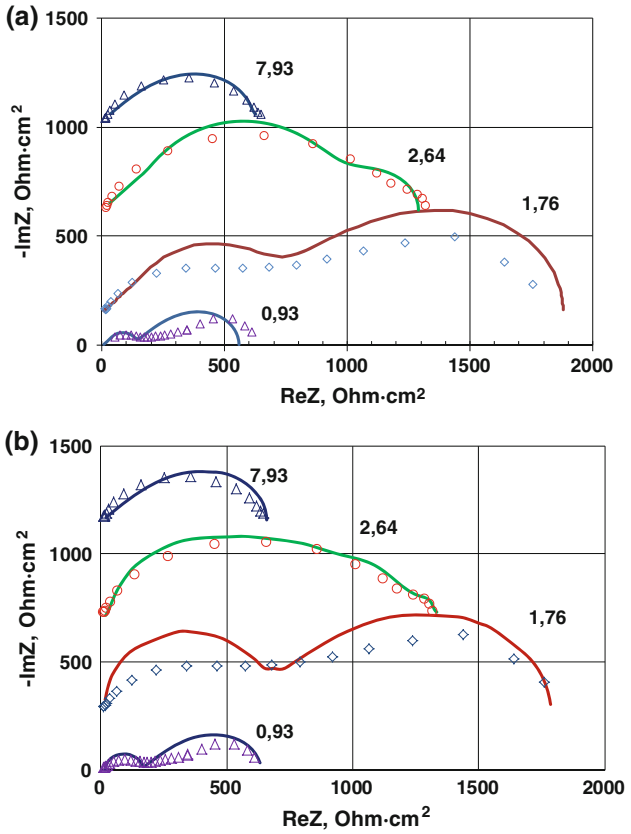

Fig. 10 Electrochemical impedance spectra for asymmetric bipolar membrane with CEL thickness of 30 microns. **a** simulation without Z_{sp} element, **b** simulation with Z_{sp} element. Concentrations of the solutions on both sides of the membrane are equal to 0.5 M. The numbers next to the curves—the value of direct current density applied to the membrane. Points—experimental data; curves—a simulation on the proposed equivalent circuit. The spectra are shifted vertically relative to each other for better clarity

Table 4 Calculated values of the fitting parameters

Scheme	i, mA/cm^2	χ, s^{-1}	R_b, Ohm cm^2	R_{wd}, Ohm cm^2	C, μF	$D_{Cl^-} \times 10^{10}$, m^2/s
With Z_{sp}	0.93	0.66	445	181	0.73	2.9
	1.76	4.56	1185	579	0.71	1.2
	2.64	287	767	543	0.7	1.9
	7.93	5032	647	–[a]	–[a]	0.8
Without Z_{sp}	0.93	2.16	624	–	–	2.6
	1.76	19.9	1759	–	–	1.5
	2.64	937	1296	–	–	1.9
	7.93	4922	652	–	–	0.8

[a] Not defined

catalytic reactions (Eqs. (7) (9)), deviations of hydrogen and hydroxyl ions concentration profiles from their steady state values are counteracted in a short period of time in a range well below the experimental observations (1 MHz) [28], and influence of the capacitive component usually refers to the frequency of the order of 1 MHz. However, due to weak catalytic activity of the studied membrane, the frequency range shifts toward frequencies of order of 1,000–100 Hz. It is the same frequency range where Gerischer impedance shifts from linearity.

An increase in the effective water dissociation constant (χ) with current density increase appears due to high co-ion leakage at low currents, which suppresses the water dissociation reaction. Comparison of the obtained constants in both cases shows that in the case when we ignored impedance of the space charge region, the constants are somewhat higher at low current densities; however, this difference is negligible at high current densities ($i = 7.93$ mA/cm^2) when water dissociation process becomes dominant (Table 4). The same goes to the resistance of reaction layer (R_b); however, its dependence from current density in both cases goes through maximum (as it was also shown on Fig. 5). The most interesting result comes from comparison of R_b when we consider equivalent circuit with and without space charge impedance. The obtained data clearly show that up to one half of total resistance rises from counter ions transport across space charge region. Again, this component (R_{wd}) becomes very small at high current densities.

Considering the foregoing, it can be concluded that during the treatment of the electrochemical impedance spectra of the bipolar membranes having low activity in the water dissociation reaction, it is necessary to consider both the charge transfer resistance of the space charge region and its capacitive component. The transition to current densities where water dissociation reaction becomes dominant process leads to the fact that Gerischer impedance becomes the main component of the impedance of the bipolar membrane and impedance of the space charge region neglection does not lead to significant errors in the

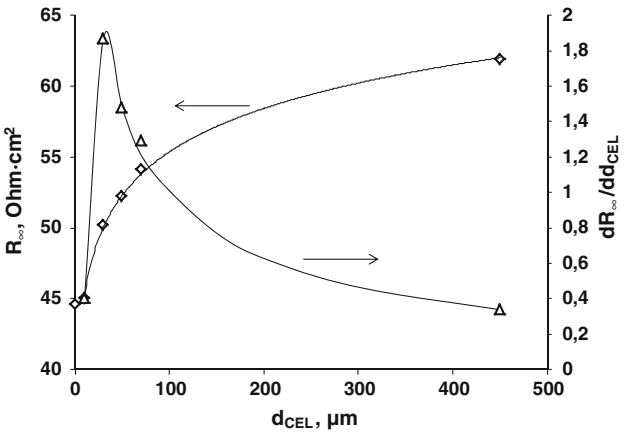

Fig. 11 Ohmic part of the electrochemical impedance of the asymmetric bipolar membranes with different CEL thickness

Table 5 Ohmic part from total membrane resistance (taking into account water dissociation reaction) measured in system of hydrochloric acid | BPM | sodium hydroxide

CEL thickness, μm	10	30	50	70	450	450 (membrane with catalyst)[a]	450 (membrane with catalyst)[b]
Ohmic part of total resistance, %	4.3 ± 2.1	3.4 ± 1.1	2.7 ± 1.4	4.0 ± 1.7	2.3 ± 0.4	81	73

Concentration of the internal solutions—0.01 M

[a] Membrane with ionpolymer water dissociation catalyst [37]

[b] Membrane with ionpolymer water dissociation catalyst [37] in 0.5 M solutions

processing of the experimental results at frequencies up to 1 MHz.

It is also interesting to note that, with increasing concentration of the external solutions, electromigration transport numbers of co-ions and water dissociation products through the membrane are virtually unchanged. For example, the electromigration transport number of hydrogen and hydroxyl ions with increasing solutions concentration from 0.01 to 0.5 M decreases from 0.86 to 0.82. In solutions with concentration of 0.5 M at low current densities, water dissociation does not occur in bipolar region and the asymmetric bipolar membrane behaves as monopolar one, however, at current density of 10 mA/cm^2, transport numbers of hydrogen and hydroxyl ions are 0.4, while in the more dilute solutions at the same current density, they are equal to 0.7–0.9. It can be concluded that at high current densities, concentration of the external solution does not matter, but at the same time, current density at which water dissociation plays a significant role in the overall mass transfer increases with the concentration of the external solutions.

3.2 CEL thickness influence on membrane total resistance

The study of electrochemical impedance spectra of the membrane reveals the contribution of different components to the total resistance. From a practical point of view, the most interesting area of research in the field of bipolar membranes is finding ways to reduce the operating voltage for the bipolar membrane. In the practical field, it can be seen that BPM total resistance is measured on the standard equipment suitable for monopolar membrane measurement. However, as can be seen from data above, this could lead a thought that the simplest way to reduce the ohmic resistance and therefore reduce the potential drop across the membrane is to reduce the thickness of the bipolar membrane. However, as it follows from the electrochemical impedance spectra of the asymmetric bipolar membranes (Fig. 9), in the absence of a water dissociation catalyst resistance of bipolar region (R_b) area may be several hundreds and at low current densities—a few thousand Ohms cm^2. At the same time, the contribution of monopolar layers resistance (R_∞) is relatively small (about 50 Ohms cm^2), even in dilute solutions.

Data analysis of impedance spectroscopy for membranes with CEL thickness varying from 10 to 450 microns is shown on Fig. 11. Obtained data clearly show that the application of a thin (10 micron) cation-exchange film hardly changes the surface resistance of the membrane. At the same time, increasing the film thickness from 10 to 30 microns leads to a jump in ohmic resistance for 5 Ohms cm^2. A further increase in the CEL thickness up to 450 microns gives even less effect, as can be seen from speed of increment in resistance with increasing CEL thickness ($dR_\infty/d\mathrm{d}_{\mathrm{CEL}}$) (Fig. 11).

The assignment of the ohmic part of the impedance to the total impedance of the membrane, comprising the resistance resulting from the water dissociation reaction in bipolar region, allows evaluating the contribution of ohmic component of the total resistance of the membrane (Table 5).

The table shows that in the absence of an effective water dissociation reaction catalyst, the contribution of ohmic part of the BPM impedance is less than 5 %. Calculated values of ohmic component of the asymmetric bipolar membranes total resistance are pretty close to each other, considering the error range. In addition, with the decrease in CEL thickness, ohmic resistance increases, due to the decrease in the electric field in the bipolar region because of the high diffusion permeability of a thin CEL for anions. At the same time, for membrane with high water-splitting efficiency ohmic resistance became the dominant part of membrane total resistance in diluted solution.

4 Conclusions

Deposition of thin MF-4SK film on the anion-exchange membrane surface leads to a sharp drop in the limiting electrodiffusion current, which is the result of bipolar border formation between CEL and AEL.

In dilute solutions, asymmetric bipolar membrane with CEL thickness of 50 microns behaves as heterogeneous bipolar membrane with CEL thickness of 450 micrometers. Even for the membranes with a thin CEL in moderately concentrated solutions, electromigration transport numbers

remain virtually unchanged, but significantly increase the contribution to the diffusion transport of salt ions.

Membranes with a thin CEL (30 microns) in moderately concentrated solutions (up to 0.5 M) show capabilities of simultaneous transport of salt ions and the generation of water dissociation products and hence can be used in processes requiring pH correction with simultaneous slight demineralization (bifunctional membrane).

Use of equivalent circuit allowed us to simplify and make more intuitive analysis of transport processes in asymmetric bipolar membrane: with increasing current density ratio of the contributions of the chemical reaction (Gerischer impedance) and electrodiffusion salt ions transport (finite Warburg impedance) shifts toward chemical reaction, and at higher current density (7.93 mA/cm^2), the water dissociation reaction in bipolar region suppresses the migration of salt ions. Starting with current density of 2.64 mA/cm^2, total resistance reduction of the bipolar membrane occurs only by reduction in electrodiffusion (Warburg part of impedance), while the contribution of the chemical reaction does not change until the current density is high enough to completely suppress salt ions transport across BPM (7.93 mA/cm^2 and higher).

Thinning of the bipolar membrane does not significantly reduce the ohmic part of the resistance, but may reduce the selectivity of the membrane. The contribution of ohmic resistance to the total resistance of the membrane (taking into account the reaction of water dissociation on bipolar border) does not exceed 5 %. Therefore, it can be concluded that the right way to reduce the operational resistance of the membrane is the selection of water dissociation catalyst.

Acknowledgments The reported study was partially supported by Russian Foundation for Basic Research, research projects No. 11-08-00718-a, 12-08-31277-mol_a.

References

1. Yua L, Guo Q, Hao J, Jiang W (2000) Recovery of acetic acid from dilute wastewater by means of bipolar membrane electrodialysis. Desalination 129:283–288
2. Novalic S, Okwor J, Kulbe KD (1996) The characteristics of citric acid separation using electrodialysis with bipolar membranes. Desalination 105:277–282
3. Alvarez F, Alvarez R, Coca J, Sandeaux J, Sandeaux R, Gavach C (1997) Salicylic acid production by electrodialysis with bipolar membranes. J Memb Sci 123:61–69
4. Persson A, Garde A, Jonsson AS, Jonsson G, Zacchi G (2001) Conversion of sodium lactate to lactic acid with water-splitting electrodialysis. Appl Biochem Biotech 94:197–211
5. Mazrou S, Kerdjoudj H, Chérif AT (1997) Sodium hydroxide and hydrochloric acid generation from sodium chloride and rock salt by electro-electrodialysis. J Appl Electrochem 27:558–567
6. Cherif AT, Molenat J, Elmidaoui A (1997) Nitric acid and sodium hydroxide generation by electrodialysis using bipolar membranes. J Appl Electrochem 27:1069–1074
7. Basta N (1986) Use electrodialytic membranes for waste recovery. Chem Eng 83:42–43
8. Kang MS, Moon SH, Park YI, Lee KH (2002) Development of carbon dioxide separation process using continuous hollow-fiber membrane contactor and water-splitting electrodialysis. Sep Sci Techol 37:1789–1806
9. Parsi EJ (1989) СПОСОБ Apparatus for removal of dissolved solids from liquids using bipolar membranes. US Patent No. 4871431
10. Bazinet L, Lamarche F, Ippersiel D (1999) Ionic balance: a closer look at the K^+ migrated and H^+ generated during bipolar membrane electro-acidification of soybean proteins. J Memb Sci 154:61–71
11. Eliseeva TV, Tekuchev AY, Shaposhnik VA, Lushchik IG (2001) Electrodialysis of amino acid solutions with bipolar ion-exchange membranes. Russ J Electrochem 37:423
12. Leitz F.B. (1971) Cationic–anionic ion-exchange membrane. US Patent №. 3562139
13. Vera E, Sandeaux J, Persin F, Pourcelly G, Dornier M, Ruales J (2009) Deacidification of passion fruit juice by electrodialysis with bipolar membrane after different pretreatments. J Food Eng 90:67–73
14. El Moussaoui R, Pourcelly G, Maeck M, Hurwitz HD, Gavach C (1994) Co-ion leakage through bipolar membranes, influence on I–V responses and water-splitting efficiency. J Memb Sci 90:283–292
15. Wilhelm FG, Pünt I, vander Vegt NFA, Wessling M, Strathmann H (2001) Optimisation strategies for the preparation of bipolar membranes with reduced salt ion flux in acid–base electrodialysis. J Memb Sci 182:13–28
16. Wilhelm FG (2001) Bipolar membrane electrodialysis. Dissertation, University of Twente
17. Ramirez P, Manzanares JA, Mafe S (1991) Water dissociation effects in ion transport through anion exchange membranes with thin cation exchange surface films. Ber Bunsenges Phys Chem 95:499–503
18. Suendo V, Minagawa M, Tanioka A (2002) Bipolar interface formation of cationic surfactant on the surface of a cation-exchange membrane: current–voltage characteristics in aqueous electrolyte solution. Langmuir 18:6266–6273
19. Sumbharaju R, Srikantharajah S, Pünt I, Stamatialis DF, Jordan V, Wessling M (2007) Asymmetric bipolar membrane: a tool to improve product purity. J Memb Sci 287:246–256
20. Melnikov SS, Shapovalova OV, Sheldeshov NV, Zabolotskii VI (2011) Effect of d-metal hydroxides on water dissociation in bipolar membranes. Pet Chem 51:577–584
21. Heterogeneous ion-exchange membranes. http://n-azot.ru/download/product/product_348.pdf. Accessed 15 Jan 2013
22. Kovalchuk VI, Zholkovskij EK, Aksenenko EV, Gonzalez-Caballero F, Dukhin SS (2006) Ionic transport across bipolar membrane and adjacent Nernst layers. J Memb Sci 284:255–266
23. Pat. US No. 5221455
24. Simons R (1993) Preparation of a high performance bipolar membrane. J Memb Sci 78:13–23
25. Zabolotskii VI, Shel'deshov NV, Gnusin NP (1979) Impedance of MB-1 bipolar membranes. Elektrokhimiya 15:1488
26. Umnov VV, Shel'deshov NV, Zabolotskii VI (1999) Current–voltage curve for the space–charge region of bipolar membrane. Russ J Electrochem 35:871–878
27. Onsager L (1934) Deviations from Ohm's law in weak electrolytes. J Chem Phys 2:599
28. Hurwitz HD, Dibiani R (2004) Experimental and theoretical investigations of steady and transient states in systems of ion exchange bipolar membranes. J Memb Sci 228:17–43
29. Strathmann H, Krol JJ, Rapp H-J, Eigenberger G (1997) Limiting current density and water dissociation in bipolar membranes. J Memb Sci 125:123–142
30. Greben VP, Pivovarov NY, Kovarskii NY, Nefedova GV (1978) Influence of ion-exchange resin nature on physic-chemical properties of bipolar membranes. J Phys Chem 52:2641–2645

31. Simons R (1984) Electric field effects on proton transfer between ionizable groups and water in ion exchange membranes. Electrochim Acta 29:151–158
32. Simons R (1985) Water splitting in ion exchange membranes. Electrochim Acta 30:275
33. Helferich F (1965) Ion-exchange kinetics. J Phys Chem 69:1178–1187
34. Gerisher H (1951) Wechselstrompolarisation von Elektroden mit einem potentialbestimmenden Schritt beim Gleichgewichtspotential. Z Phys Chem 198:256
35. Macdonald JR (1953) Theory of ac space–charge polarization effects in photoconductors, semiconductors, and electrolytes. Phys Rev 92:4
36. Stoynov ZB, Grafov BM, Savova-Stoynov BS, Elkin VV (1991) Electrochemical impedance. Translated from Russian. Nauka publishing, Moscow
37. Shel'deshov NV, Krupenko ON, Shadrina MV, Zabolotskii VI (2002) Electrochemical parameters of heterogeneous bipolar membranes: dependence on the structure and nature of monopolar layers. Russ J Electrochem 38:884